Final Report—May, 2006
Report Number DOE/NA/00069-Final

Reporting Period: Dec. 15, 2002 to Feb. 28, 2006

DOE-NNSA Project DE-FG03-03NA00069

Micro and Nano-structure Development and Multiscale Physics at Sliding Metal Interfaces

PI: D. A. Rigney, The Ohio State University,
in collaboration with Los Alamos National Laboratory

Introduction and Background:

Much work has been reported on the response of ductile materials to high strain rates during impact. Separately, much work has been reported on sliding friction at various sliding velocities. This project is concerned with a combination of these conditions and the response of ductile materials to extreme loading conditions such as those involved in impact loading with sliding friction.

The work involves collaboration of the tribology group in Materials Science and Engineering at OSU and two groups at LANL, an impact loading group in the dynamic experimentation division and a computer simulation group in the applied physics division. The work includes impact and sliding tests, materials characterization and computer simulation. More recently, the OSU group has supplemented that work with analysis using continuum mechanics. The two teams are investigating the same materials pairs: Cu/Cu, Al/stainless steel (SS) and Ta/Al. These were selected to allow comparison with the results of computer simulations at LANL and with sliding tests at OSU. The LANL team has provided impacted specimens for characterization at OSU. Both teams are performing molecular dynamics (MD) simulations to help guide and interpret the experimental work.

Summary of timeline: The project grant announcement was made on August 30, 2002. The award papers were received at OSU on February 3, 2003, with an official project start date of Dec. 15, 2002. The OSU team was assembled during autumn, 2002, and planning and preliminary work began before the official start date. The four members of the Los Alamos (LANL) team visited OSU on November 15, 2002, for a full day of discussions, lab tours and project planning. The first test samples were sent by LANL to OSU in December 2002. One member of the OSU team worked at LANL during the summer of 2003. The OSU team visited the LANL lab early in 2004, and one member returned for a more extended visit late in 2004.

Project personnel:

At OSU: D. A. Rigney, PI; K. Subramanian (post-doc); A. Emge and H. J. Kim (PhD candidates). H. J. Kim came to us with an M.S. in Materials Science and Engineering. He has

passed the written and oral parts of our PhD candidacy exam. A. Emge came to us with a B.S. in Chemistry. He passed the PhD candidacy exam early in 2006. Kim is focusing on the aluminum part of the project, especially the effects of environment, while Emge is focusing on copper, especially effects of strain rate. K. Subramanian assisted the two students with structural and chemical characterization, including TEM preparation and analysis. He was also involved in theory and computer simulations. He left OSU in Sept., 2005, to become an Assistant Professor at IISc, Bangalore, India. We continue to collaborate with him.

At LANL: P. Rightley (Mech. E.); J. Hammerberg (Physics, theory); P. Crawford (MSE). PR and PC have focused on the tests of impact with sliding; JH has focused on MD simulations of sliding for relevant materials pairs at different sliding speeds.

Coordination of OSU and LANL Teams: Coordination among the interdisciplinary team members was accomplished via email, telephone, discussions at conferences and at a DOE workshop in Albuquerque, and by visits of Rigney, Kim, Emge and Subramanian to LANL. The shut down of LANL and subsequent organizational changes there postponed other planned visits. However, in response to our petition, operations in the impact lab did resume, and Emge was able to have an extended visit in Dec., 2004.

Experiments at LANL:

The team members at LANL supplied some of the tested specimens characterized at OSU (others were produced and tested at OSU). The experiments at LANL involved an improved rotating barrel gas gun (RBGG) that allows independent control of impact velocity and sliding speed. The RBGG has the ability to provide consistent wave profiles with short rise times under high speed sliding and high impact load conditions. Unfortunately, test results showed that the mechanical joint configuration does not completely transfer the shear load through the joint interface, resulting in incorrect values for the coefficient of friction during impact and sliding events. The epoxy joint configuration appears to transfer the complete axial and shear load through the joint. However, the measured shear stress exceeds the specified maximum shear stress for the epoxy. This limits the sliding speeds that can be tested in this condition.

Average values for the coefficient of friction of 0.5 for the "no sample" configuration agree with published data on copper/copper tribo-pairs. The lower values for the epoxy and mechanical joint configurations suggest that the test configuration does have an effect on the coefficient of friction. The next step is to test the OFHC Cu/Cu tribo pairs at various combinations of sliding speed and impact load to determine the behavior of the coefficient of friction. Other tribo pairs (Al/SS, Al/Ta) will be investigated in a similar fashion. Tests performed at the extremes of the RBGG—low sliding and axial speeds, high sliding and axial speed—exhibited similar time average coefficients of friction of about 0.2. The lower value may be a result of a lower surface roughness of the impact surface. Design of RBGG II—a second generation RBGG—is underway. This new design uses the same conceptual design with a different physical design approach. An air impulse turbine will be used as the mechanism for rotation of the barrel, allowing rotational sliding speeds of up to 350m/s (50,000 rpm).

Inspections that followed the LANL shut-down identified the need for small changes in the

RBGG facility. These changes have been made. They mainly involved covering electrical connections and providing proper documentation for all electrical components. No changes in the operation of the RBGG were needed.

Modifications in the target rod/projectile alignment system are in progress. These are designed to reduce or eliminate additional impacts after the initial impact. This is expected to facilitate production of test specimens needed by the members of the OSU team for continuing characterization work.

Experimental Progress at OSU:

Brief Summary of Experimental Progress at OSU:

The OSU portion of this research project focused on the frictional behavior and structural changes in ductile FCC metals subjected to impact loading with sliding. The OSU group examined samples tested in LANL's novel RBGG and compared them with samples produced at lower sliding speeds at OSU. The group also worked with Dr. R. Winter and Mr. P. Keightley at AWE (Atomic Weapons Establishment), Aldermaston, UK, and examined a specimen from their explosively driven testing of impact with sliding. The experimental work has included comparisons of specimens tested in different environments (air, changes in humidity, vacuum). Other work by the OSU group involved molecular dynamics (MD) simulations and analysis by continuum mechanics.

The experimental work at OSU focused on three tasks: (1.) designing and building an improved system for sliding tests at intermediate velocities, (2.) developing appropriate pre-testing surface preparation and (3.) developing post-test characterization techniques. The new pin/disk wear testing system can achieve sliding speeds up to 1 m/s in a range of environments and contact times as small as 0.1 s. Resolution has been improved from +/- 7 grams to better than +/- 1 gram. Transmission Electron Microscopy (TEM) was done on cross-sections of the as-machined annular OFHC copper samples. This revealed substructures consistent with extensive subsurface damage. These features would complicate our efforts to study the changes produced by impact with sliding. Samples should have a minimal amount of subsurface deformation prior to testing, so the deformation due to sliding will not be obscured. Therefore, a study was conducted to find a test specimen preparation method that would minimize subsurface deformation. Three machining methods were analyzed: lathe turning, fly-cutting and electrical discharge machining (EDM). Post-machining annealing at 275C for one hour in a vacuum furnace was also performed to remove deformation remaining from the machining processes. Microhardness was measured as a function of the distance from the machined surface. This was a simple way to determine the extent of subsurface deformation. The results show that annealed fly-cut samples are best for our purposes. Similar tests on pure aluminum samples suggest that annealing of fly-cut samples at 260C for an hour is sufficient to remove subsurface deformation. Subsequent chemical polishing removed surface layers and provided a clean surface.

Sliding tests with prepared copper specimens were performed in air at sliding speeds ranging from 5 to 50 cm/s. Steady state values of friction coefficient are similar for different velocities, but the sliding distance required to achieve steady state is longer at higher velocity.

Also, at the highest speed, the steady state friction is lower, probably because of thermal effects. Material transfer was observed but mixing in of oxygen was not a major influence because test times were short. TEM revealed a nanocrystalline layer on the surface, as expected. Tests on aluminum were performed in air, nitrogen and vacuum for a range of sliding speeds and normal loads, and samples were characterized by SEM/EDS, XPS and TEM. Oxygen progressively mixes into the deforming surface material and influences the evolution of surface chemistry, topography and friction. In vacuum, these effects are reduced and the friction is modified. It is higher than in air initially, but as sliding continues, the trend is reversed. Preliminary TEM results for short time testing show that the grain structure is refined through deformation and mixing. There is also evidence of a surface amorphous layer produced by sliding.

Detailed Description of Experimental Progress at OSU:

Equipment Upgrades

OSU Pin-on-Disk System: The existing pin-on-disk test apparatus was modified to improve the resolution and reliability of the normal load data acquisition system. The previous set-up consisted of a single strain gage in a quarter bridge configuration. The previous location of the normal load strain gage was close enough to the contact between the pin and disc that the strain gage output was suffering from thermal effects. This caused irregular loading profiles during tests. Two steps were taken to reduce this source of error. First, the pin holder was redesigned to increase its mass so that it will act as a heat sink between the contact area and the strain gages. A third pin mounting position was added to allow tests to be performed at higher velocities. Secondly, the quarter bridge strain gage was replaced with a half-bridge configuration. This has the advantages of increasing the resolution from ±7 g to less than one gram, and also has the ability to cancel thermal effects. The normal load strain gage plate was also redesigned to increase the resolution of the normal load. This was done by moving the gages further from the contact area and by reducing the thickness of the plate. The method of calibration was also improved.

Kelvin Probe Installation: A Kelvin Probe (KP) was installed on the horizontal pin-on-disk tribometer. The pin holder was redesigned so that the KP tip could be positioned over the wear track while giving adequate clearance between the KP tip and the pin holder. The KP is mounted on a micrometer driven linear stage with independent XYZ translations that allows for precise and repeatable positioning of the KP. A dual output DC power supply was purchased and installed to power the KP.

Cold Trap Addition: A liquid nitrogen cooled foreline trap was added to the vacuum system to prevent back streaming of oil from the mechanical pump into the system and to reduce pumping times.

Los Alamos National Laboratory Visit

Andrew Emge visited LANL in December 2004. During this extended visit he viewed the RBGG and became familiar with the set-up. He also took an electrical safety course that is required before he could be allowed to operate the RBGG. He also completed the required paperwork for a clearance level that would allow him to take additional required safety courses

on the internet so he would not have to take them during future visits and would instead be able to focus on operation of the RBGG. Andrew also met with Paula and Kevin to discuss their plans for a next generation RBGG that would utilize air bearings and be capable of much higher rotational velocities.

Copper on Copper Tests

Friction tests were performed on OFHC copper sliding against OFHC copper with both the pin-on-disk and rotating barrel gas gun (RBGG) tribometers. The sliding velocity for these tests ranged from 0.05 m/s to 5.2 m/s. The pin-on-disk tests were run for a total sliding distance of 30 m under an applied load of 100 g. The RBGG tests were all fired at an axial velocity of 12 m/s.

Surface Preparation Changes: Additional surface preparation steps were added in order to remove machining marks from the flycutting process. After flycutting, the samples are mechanically polished sequentially with 400, 600, 800 and 1200 grit SiC polishing papers. After annealing, the surfaces are chemically polished followed by ultrasonic cleaning in methanol. The samples are cleaned with compressed air prior to testing.

Pin-on-Disk Tests (copper): Oxygen free high conductivity (OFHC) copper disks were tested in sliding against 440C stainless steel balls. The tests were performed at varying sliding speeds ranging from 5 cm/s to 50 cm/s with contact times as short as 0.1 second. The tests were all performed in an air atmosphere. The applied load was held constant with a 200 g counterweight, which translates to roughly 100 g at the pin. The sliding times were adjusted to achieve a fixed sliding distance of 30 m for all tests. The rotational velocity of the disk is adjusted to achieve the desired sliding velocity before the pin is brought into contact so that initial transients can be measured.

Surface changes and deformation resulting from sliding were characterized with the use of scanning electron microscopy (SEM) and energy dispersive X-Ray spectroscopy (EDS). Deformation has been observed on the surfaces of both the pin and disk accompanied by material transfer from the disk to the pin. Subsurface deformation was studied with the use of Transmission Electron Microscopy (TEM). Focused Ion Beam (FIB) milling was used to prepare site-specific TEM foils from the wear track.

Friction Data Analysis (Copper): Friction force results from four tests are shown in Figure 1. The steady state values are very similar for all but the highest velocity test, for which the friction force is lower. The main difference between the results for the three lower velocities is that the sliding distances required to achieve steady state values change with sliding velocity. From Figure 1 it can be seen that the distance required for steady state increases as the sliding velocity decreases.

Characterization (Copper): Once the tests were performed, Scanning Electron Microscopy (SEM) with Energy Dispersive Spectroscopy (EDS) capabilities was used to characterize the sliding surfaces on both the pin and the disk. SEM and EDS results did not show material transfer from the pin to the disk, but did show material transfer from the disk to the pin as can be seen in Figure 2(a). This is expected as the pin is the harder of the two materials. EDS (Figure 2(b)) was also used to determine the extent of oxidation on the wear track on the disks.

EDS detected only a couple of atomic percent oxygen on the wear track from each test.

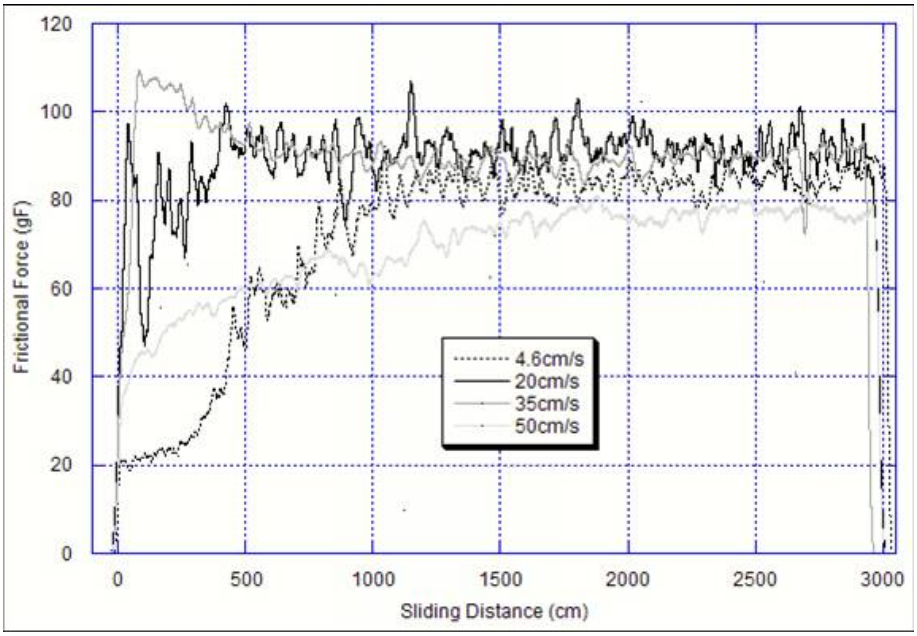

Fig. 1: Friction force vs. sliding distance for four sliding velocities. Note steady state values, especially at the higher value of 50 cm/s.

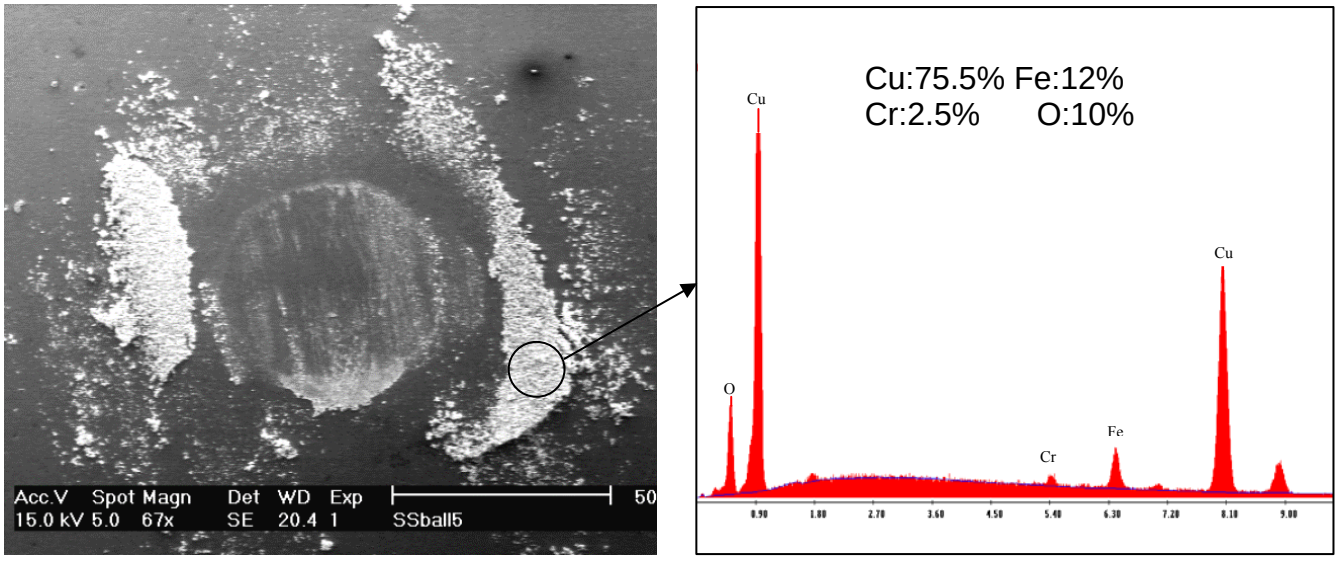

(a) (b)

Fig. 2: (a) SEM image of a 440C stainless steel ball after sliding against an OFHC copper disk at 4.6 cm/s for 30 m. (b) EDS of the wear debris shows a large percentage of copper signifying material transfer from the disk to the pin.

The width of the wear track on the disks is very similar for all of the tests at about 300-400 μm. A corresponding worn area could also be seen on the balls with a width very similar to that of the track on the disk. The wear track morphology varies with a change in sliding velocity. At the low velocity of 4.6 cm/s the grooves in the wear track are almost entirely circumferential. As the sliding velocity increases, some of the grooves on the wear track turn away from the circumferential direction and move across the wear track as shown in Figure 3 from the 50 cm/s test. These grooves are seen to increase in frequency as the sliding velocity increases.

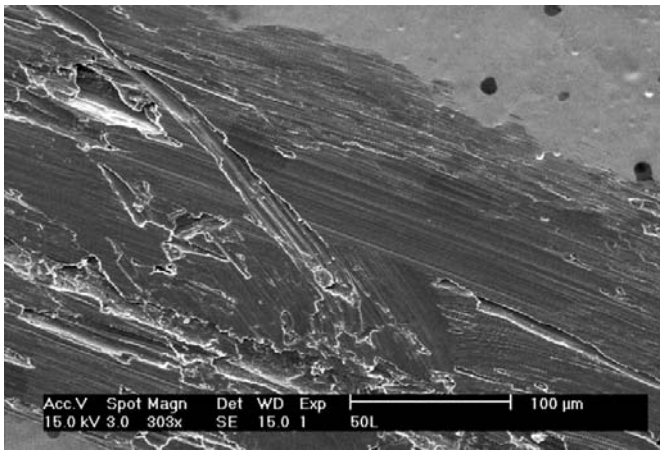

Fig. 3: Wear track on OFHC copper disk after sliding against 440C stainless steel at 50 cm/s for 30 m.

Subsurface deformation of the worn disk surfaces was studied with Transmission Electron Microscopy (TEM). Focused Ion Beam (FIB) milling was used to prepare site-specific TEM foils from the wear track in the longitudinal direction. The TEM revealed a nanocrystalline layer that extends about 0.5 μm below the surface (Figure 4). Below this layer is a heavily deformed region with larger grains.

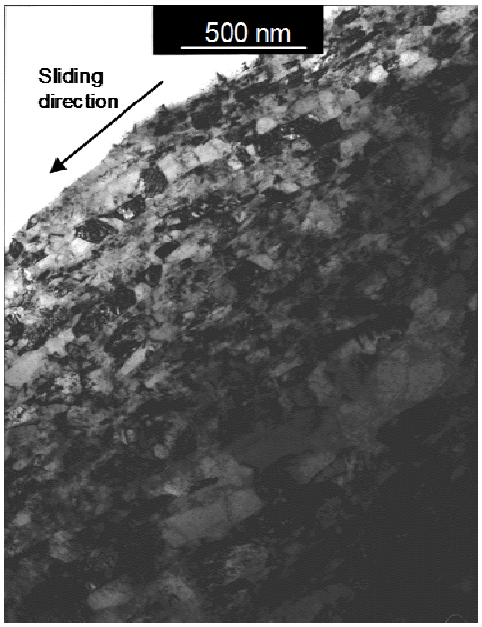

Fig. 4: TEM image of OFHC copper sample showing a nanocrystalline region produced by sliding against 440C stainless steel in air.

RBGG Samples: One pair of target and projectile rods was received from LANL in 2004. The pair was from a Cu/Cu test at the minimum axial and rotational velocities. The projectile was spun at 1500 rpm and fired with a 20 psi plenum pressure. Optical and scanning electron microscopy did not reveal a clear wear track on the projectile or on the target. However, there were some circumferential scratches on the projectile. EDS showed a low amount of oxygen on the surfaces.

The shut-down at LANL stopped production of RBGG specimens for the second half of 2004 and into 2005. Several new specimens were produced during February and were received at OSU in early March 2005. These were produced at high impact and rotation velocities, so our expectation was that changes in the material would be more dramatic. The results from these tests are included in the plot of friction, shown in Figure 5. The friction coefficient in air (~30% relative humidity for pin-on-disk tests) was found to be fairly constant at both the low and high sliding velocities, but it is lower for the higher sliding velocity tests.

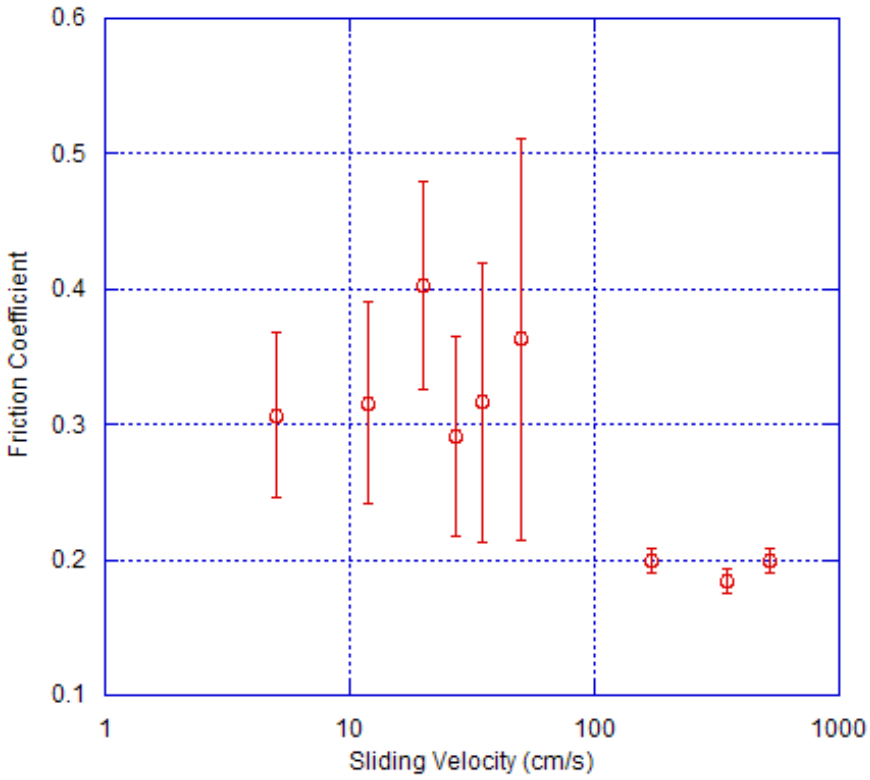

Fig. 5: Friction coefficient vs. sliding velocity in air for both pin-on-disk and rotating barrel gas gun (RBGG) tests of OFHC copper sliding against OFHC copper.

The surface and subsurface deformation induced by sliding was characterized by SEM with EDS and by TEM on the disks from the pin on disk tribometer and on the projectiles from the RBGG tribometer. SEM results showed significant wear on the projectile surfaces as seen on Figure 6. The wear track was found to be more pronounced nearer the center of the projectile (inner part of curved track). SEM of the disk surfaces showed discontinuous wear tracks as

seen in Figure 7. EDS showed less than 5% oxygen on all of the surfaces and wear tracks. This was expected because of the short time of contact. At longer sliding times, the process of mechanical mixing can raise the oxygen content.

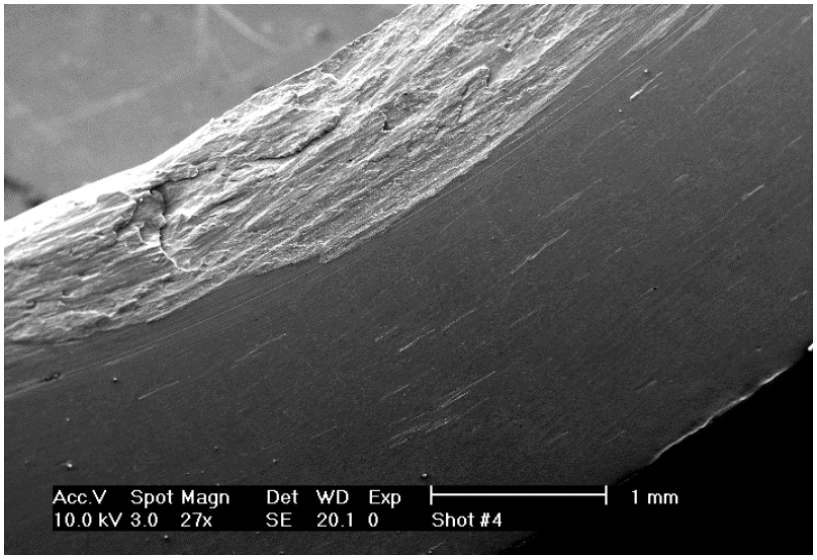

Fig. 6: SEM image of the surface of an OFHC copper projectile after sliding at 5.2 m/s against an OFHC copper target. The wear track is more developed near the inner edge of the projectile (upper edge in the image.

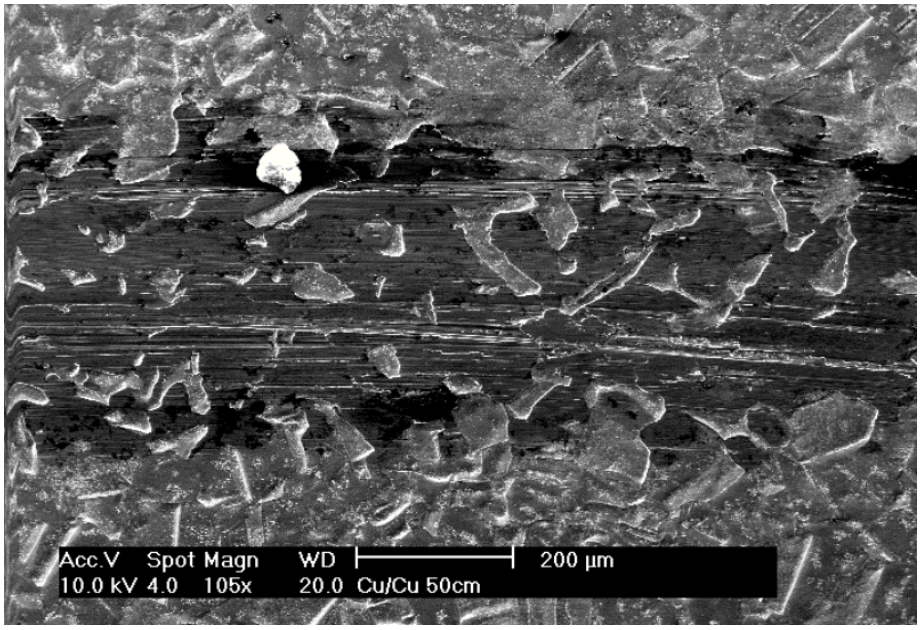

Fig. 7: SEM image of an OFHC copper disk surface after sliding against a copper pin at 0.5 m/s for 30 m under an applied load of 100 g.

Focused ion beam (FIB) milling was used to produce site-specific TEM samples. TEM results from just below the sliding surface of the projectiles show heavy deformation indicated by aligned microstructure and nanocrystalline regions (Fig. 8).

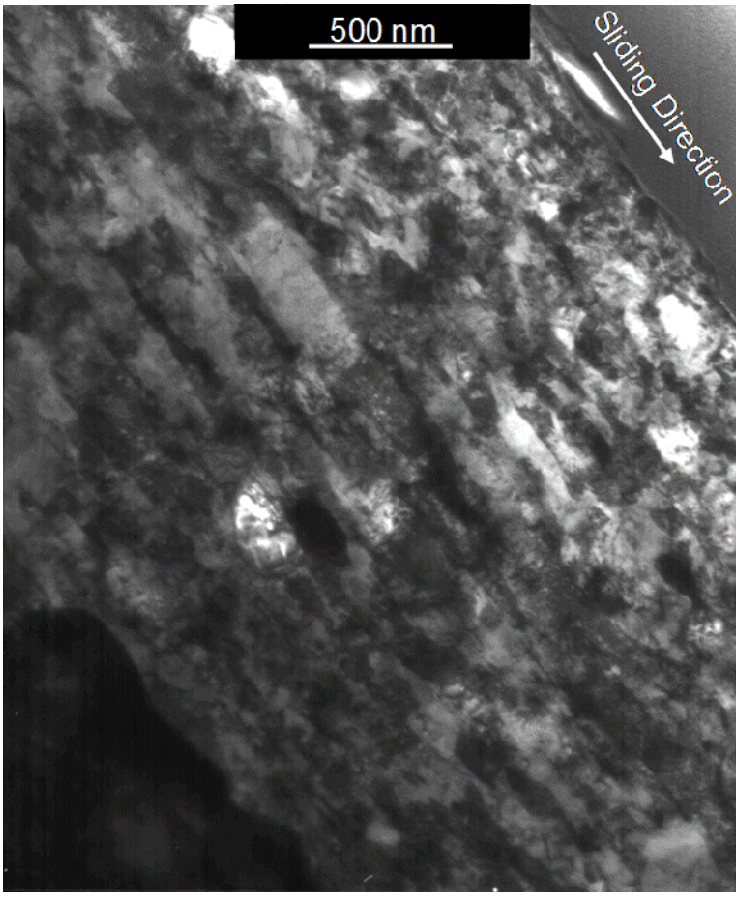

Fig. 8: Bright field TEM image of the subsurface region just below the sliding surface of an OFHC copper projectile after sliding at 5.2 m/s against an OFHC copper target.

Surface Preparation of AWE Copper Samples: Four OFHC copper samples were received from AWE for surface preparation. The surfaces were mechanically polished with 400, 600, 800, and 1200 grit SiC polishing papers. They were then annealed in a vacuum furnace at 275°C for one hour. Finally, the surfaces were chemically polished, and the samples sent back to AWE for testing.

Sliding Tests (Aluminum)

The improved tribometer can achieve sliding velocity up to 1 m/s and with contact as short as tenths of a second. Therefore, the equipment can bridge the gap between the RGBB apparatus at LANL and the more conventional pin-disk tribometer. Sliding speeds ranged from ~ 25 cm/s to ~ 50 cm/s and contact time was about 1 second. Normal load was increased to 150 g, which is three times larger than used for earlier low speed tests. Vibrating of the arm system in

the tribometer causes the data signal to oscillate as shown in Figure 9(a). After choosing a proper contact time, the signal was filtered by a numerical smoothing process. Figure 9(b) shows the processed signal. The processed experimental data are summarized in Figure 6. Microstructure characterization will be done next. As shown in Figure 10, frictional behavior is similar regardless of sliding speed in this range. Friction coefficient values are about 0.4 except during the initial and final transients. This is less on the average than the values obtained during long-time and low speed sliding tests. This is consistent with several authors' results, which indicate a reduction in the coefficient of friction when the normal pressure and/or the sliding velocity are increased.

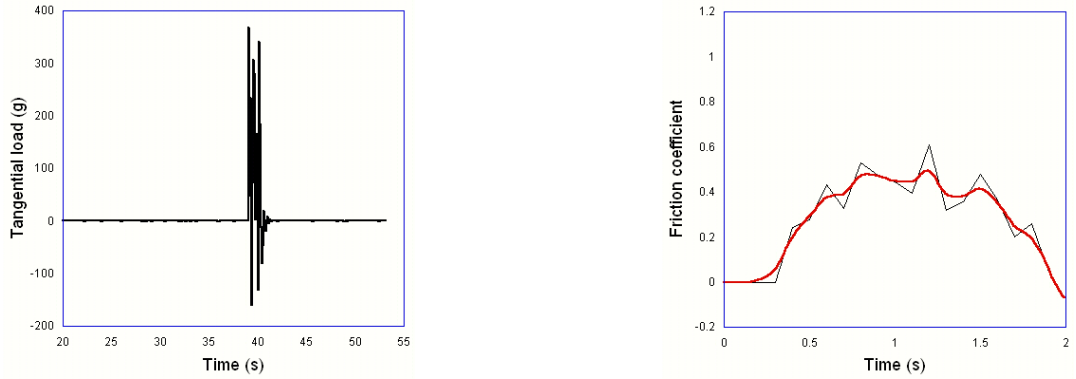

(a) (b)

Fig.9: (a) Original tangential load signal and (b) friction coefficient after data processing

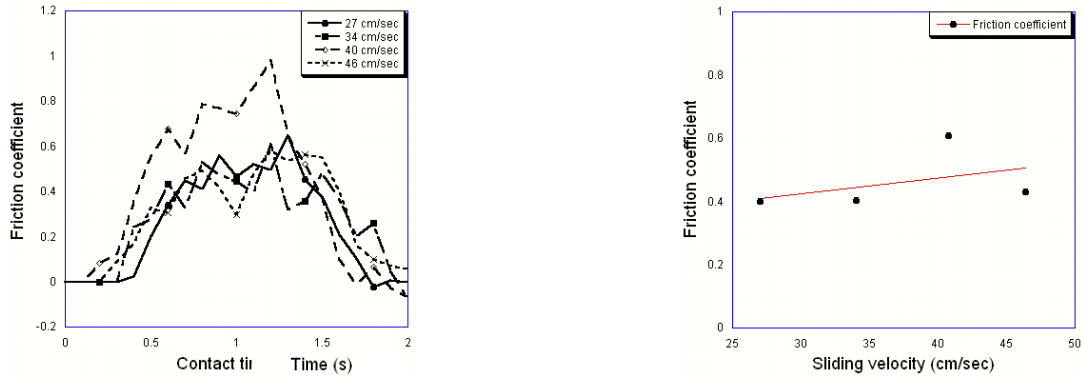

Fig.10: Friction coefficient for impact-like sliding.

Environmental Effects (Aluminum): Initial sliding tests were in air. Testing conditions were then extended to nitrogen and to air with different humidities. After five hours of sliding, the wear surface and wear debris were characterized using SEM and EDS. Friction coefficients are shown in Figures 11(a) and 11(b) for different humidities. In both cases, the friction coefficient decreases at first and then increases. However, the time needed to reach the lowest value is not the same. With high humidity, the friction coefficient quickly decreased; at low humidity, the rate of decrease was much less. Sliding behavior is similar in vacuum and in nitrogen (Figures 11(c) and 11(d)). While tests in air showed distinctive regimes of friction, tests in vacuum and nitrogen showed more steady friction.

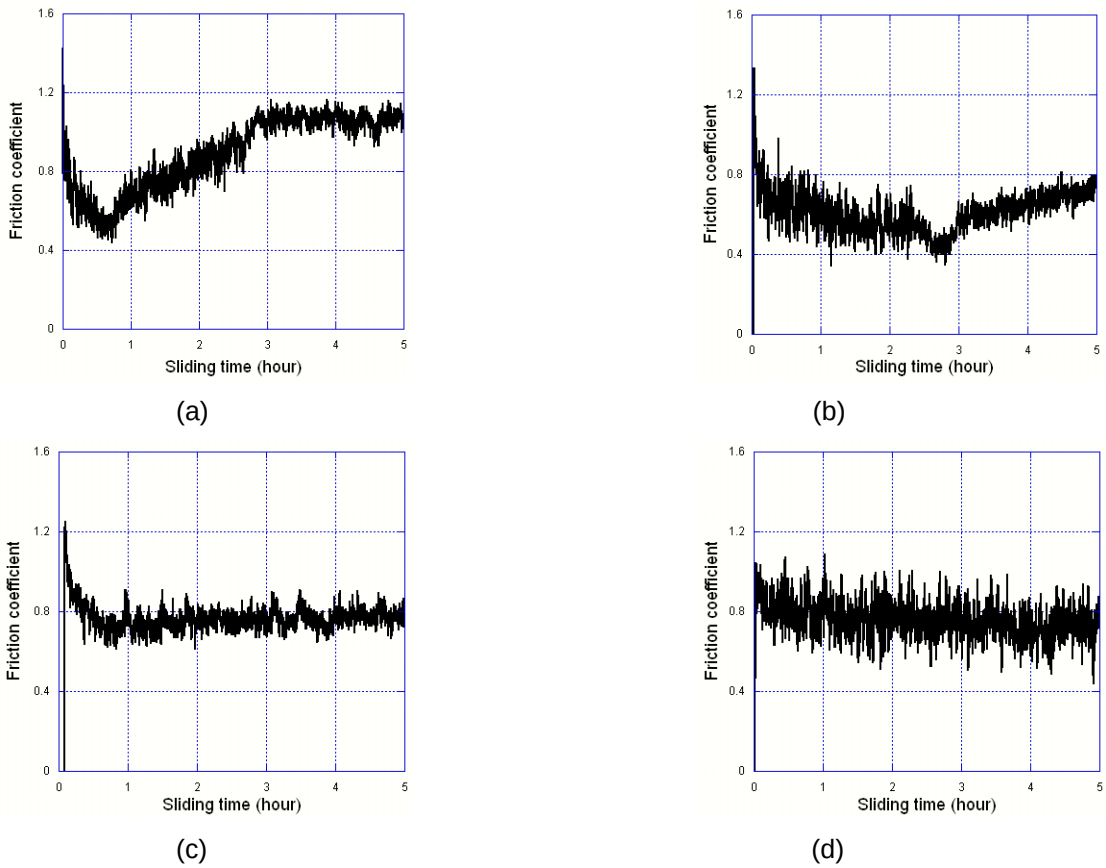

Fig.11: Friction coefficient for different environment tests. (a) Air and high humidity (RH=60%); (b) Air and low humidity (RH=20%); (c) Vacuum; (d) Nitrogen

Figure 12 shows SEM images of the sliding surface for each case. Clear differences in wear track morphology are visible; they depend on the extent of oxidation. EDS confirms that more oxygen is incorporated in or on the surface for sliding with high humidity. The wear track width is the smallest for the vacuum environment test. The wear surface for the vacuum test shows smooth areas on the surface. After sliding in the nitrogen environment, the wear track morphology is very rough and the track width is larger than in the other cases. This is consistent with the large fluctuations observed in the friction force data.

In Figure 13, SEM images of wear debris are shown. The test in vacuum produced a very small amount of wear debris. The higher the oxygen level, the smaller the debris size is. In air tests, aluminum debris with more oxide ranges in size from a few tens of nanometers to micrometers.

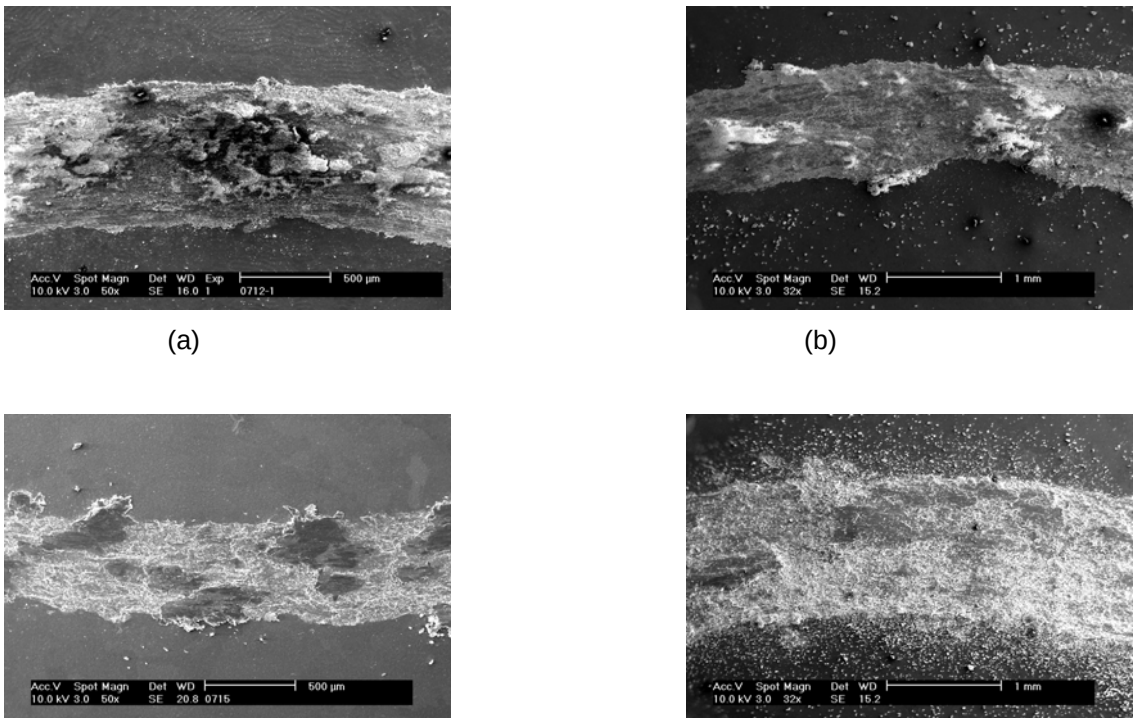

Fig.12: SEM images of wear track for different environment tests. (a) Air and high humidity (60%); (b) Air and low humidity (20%); (c) Vacuum; (d) Nitrogen

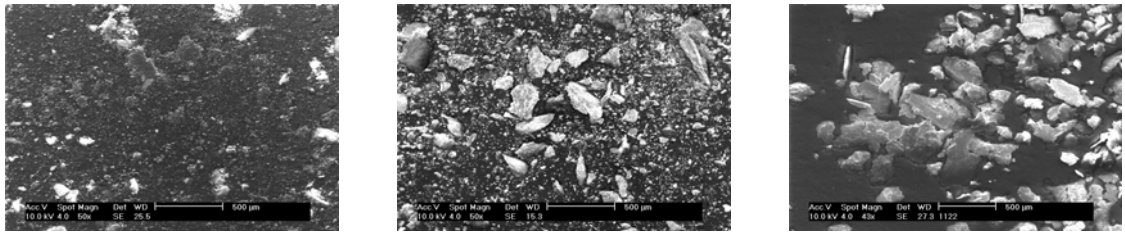

Fig.13: SEM images of wear debris for different environment tests. (a) Air and high humidity (60%); (b) Air and low humidity (20%); (c) Nitrogen

There have been many proposed mechanisms of oxide particle debris formation. The model most widely used is based on growth of a surface oxide followed by removal of the oxide as debris. Earlier work in the OSU group has never shown support for this model. In general, the debris particles are mostly metallic with an intimate mixture with oxygen, consistent with a mechanism involving mechanical mixing. Further characterization is needed to establish the mechanism operating in the present case.

Friction coefficient and wear rate as a function of relative humidity are summarized in Figure 14. For an aluminum and steel tribopair, the friction coefficient decreased initially. However rate of the decrease was different in different environments. In (a), a schematic of the friction coefficient is presented. In a high-humidity environment, the friction coefficient decreased

faster than under less humid conditions. Surface hydroxide may prevent direct contact between the sliding materials. This would explain why the friction coefficient is lower when sliding with more water present. In (b), the wear behavior is shown for different levels of relative humidity.

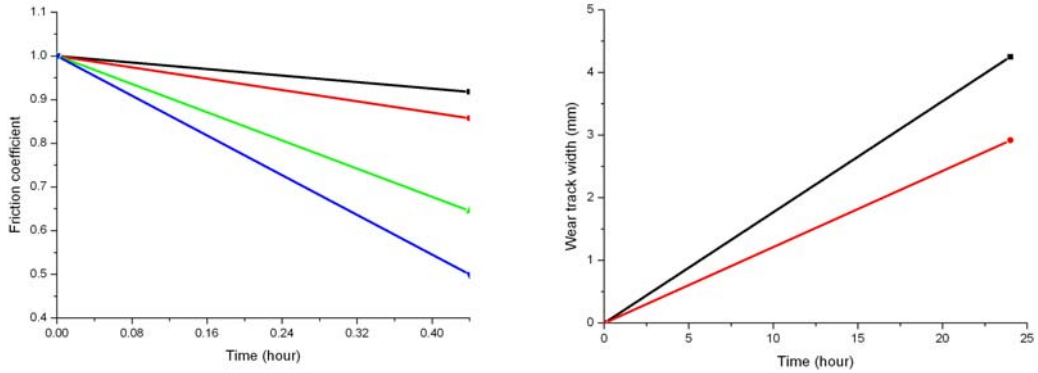

(a) (b)

Fig. 14: (a) Approximate trends of friction coefficient vs. time for four levels of relative humidity (20%, 46%, 60%, 95%, top to bottom); (b) approximate trend of wear track width for two levels of relative humidity (30%, upper; 95% lower)

In these experiments, weight change was too small to represent wear rate, so wear track widths were compared instead of weight changes. After 24 hours of sliding, the track width in a high-humidity environment was smaller than with less humidity. Again, surface hydroxide seems to be responsible for reducing the wear rate.

After 24 hours of sliding, wear debris was collected and characterized by SEM with EDS. The shapes of the wear debris particles are shown in Figure 15(a). They are mostly equiaxed and some particles are less than 100 nm diameter. As sliding time increases, the sizes of debris become smaller and more uniform. The shape and size of the wear debris indicate a similarity between sliding friction and mechanical alloying. EDS data are shown in Figure 15(b). The wear debris exhibit a high concentration of oxygen. The oxygen content varies in different regions because the wear debris were collected at the end of sliding and consist of particles from produced at all stages of sliding. However, at longer sliding times, the oxygen content was higher overall. Some debris particles contained as much as 70 at% oxygen, i.e., higher than in Al_2O_3.

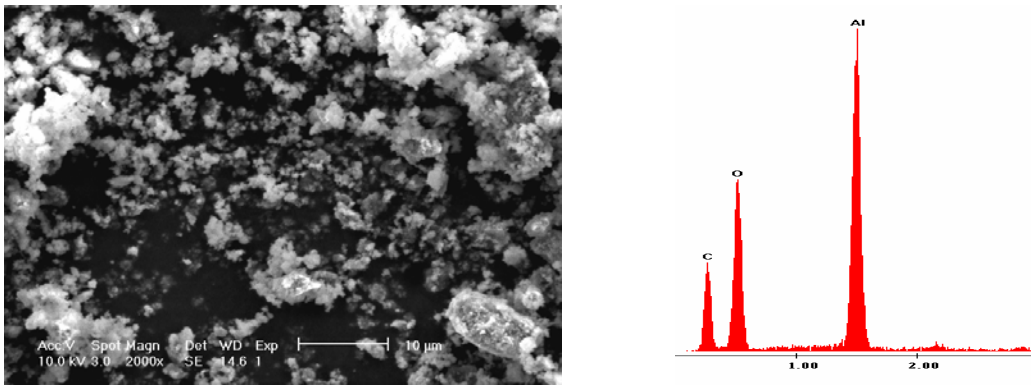

(a) **(b)**

Fig. 15: (a) Wear debris from sliding of aluminum in air. (b) Debris contains very high concentrations of oxygen, but not in the form of crystalline alumina.

XRD Analysis of Wear Debris (Aluminum): XRD (X-ray diffraction) analysis was performed to identify crystalline phases present in the wear debris. Although the wear debris contains a large amount of oxygen, XRD scans do not show a pronounced aluminum oxide peak. In Figure 16(a), the spectra from high purity aluminum powder and alumina are compared with the spectrum from wear debris. In Figure 16(b), Al (111) lines are shown for different sliding times. The Al (111) peak position from a Cu Kα source is shifted toward a lower angle, suggesting a change in lattice parameter or a large elastic strain in the wear debris. The peak shift is larger for increasing sliding time. These peak shifts indicate that the interplanar spacing for (111) is increased. Based on the XRD peak shifts, the amount of strain can be calculated with the use of Bragg's law. After 24 hours, sliding produces about 0.3% strain. However, debris generated from sliding in a vacuum environment did not show a shift of the (111) peak. In Figure 16(b), the peak position is identical to that of the original aluminum before sliding. This indicates that the strain in the debris produced in air tests was caused by oxygen. Close examinatin of the XRD peaks shows peak broadening from some combination of the particle size effect and strain gradients. As demonstrated above, the debris particle size is smaller when sliding time increases.

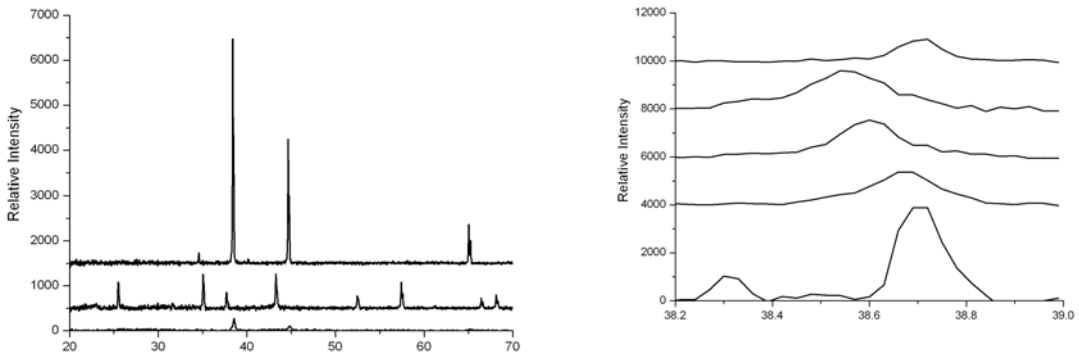

Fig. 16: (a) XRD patterns for Al, Al_2O_3 and debris (top to bottom); (b) (111) peaks for sliding times of 0, 5, 11 and 24 hours (bottom to top) in air. Upper trace is for 6 hours sliding in vacuum. The left peak at 0 hours is an artifact (SiC peak from embedded abrasive during mechanical polishing).

XPS Analysis of Wear Debris (Aluminum): XPS was used to investigate how the oxygen is distributed in the worn Al. Binding energies for the Al2p line were compared for wear debris and high purity Al powder, as shown in Figure 17. Wear debris was generated during a 24 hour sliding test. There is a substantial shift of the Al2p core level between Al metal and Al compound peaks. In this Figure, the Al metal peak position could be aligned for calibration purposes, because the wear debris contained some Al metal pieces that were generated during the early stages of sliding. The XPS results show that the aluminum compound binding energy for the wear debris and the Al powder are different, indicating that oxygen in the wear debris is combined with Al differently than in alumina. The higher binding energy and the higher oxygen content in the debris suggest that Al hydroxide has formed. It is known that hydroxides of aluminum, such as boehmite (γ -AlOOH), have higher Al2p binding energy than in alumina.

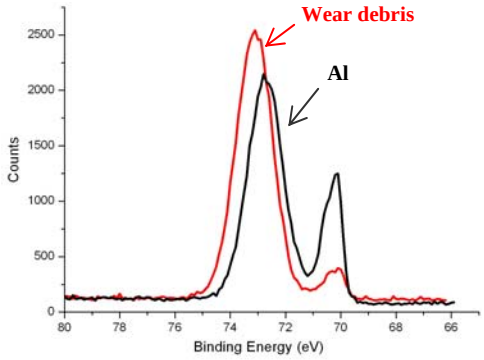

Fig. 17: Al2p XPS peaks for wear debris and high purity aluminum powder (with surface oxide), showing a clear shift of binding energy for the higher energy "oxide" peaks.

TGS and DSC Analysis of Wear Debris (Aluminum): To determine whether or not hydroxide formed during sliding, TGA and DSC analyses were conducted. Figure 18(a) shows TGA plots as a function of temperature and Figure 18(b) shows DSC results. TGA monitors weight change as a function of temperature during heating. To prevent oxidation, which leads to increased weight, flowing Ar was used during the measurement. Wear debris was collected after friction tests in different humidity conditions. Overall, the wear debris lost weight, as confirmed by TGA. Wear debris tested in low humidity conditions (~30%) lost about 4% of its weight. However wear debris tested in high humidity conditions (~95%) lost about 25% of its weight. These results support the assumption of hydroxide formation at the surface of wear debris particles. The H_2O component is presumed to have evaporated during heating. In high humidity conditions, hydroxide could form more easily. DSC results showed an endothermic reaction occurred during the heating of wear debris. Thus, XRD, XPS, TGA and DSC are consistently in support of the formation of Al hydroxide during sliding of aluminum in air.

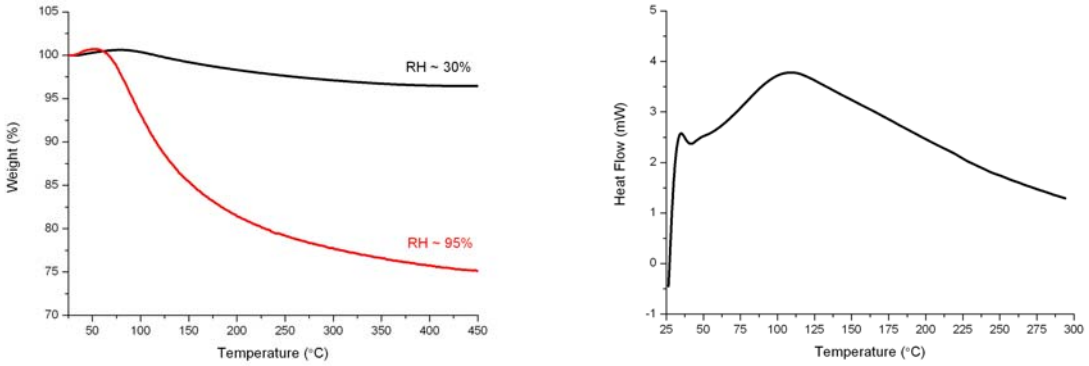

(a) **(b)**

Fig. 18: Changes suggesting the presence of H_2O or hydroxide; (a) Weight changes during TGA; (b) Endothermic transition shown by DSC.

Impact with Sliding (Aluminum)

During the LANL shut-down we obtained samples of aluminum 5083 impacted with sliding at another laboratory. These specimens allowed us to check our TEM preparation techniques and to obtain preliminary information on structure changes. Specimens were prepared for TEM first by Focused Ion Beam (FIB) and then by conventional thinning methods.

Nanostructure formation induced by severe plastic deformation has been reported frequently. The structures are produced at high strains and high strain rates. Aluminum (EN AW5083, BS EN 573-4) and stainless steel (321512 to BS EN 10088-3 [X2CrNi 18-9]) were selected as contact materials. Using novel experimental equipment, called FN6, at AWE (Atomic Weapons Establishment), Aldermaston, UK, the microstructure created by explosively driven impact with sliding could be studied. With FN6, the sliding velocity range is 60~180m/s and the contact time is 10μs. Examples of the results are shown in Figure 19(a) and (b). Based on SEM analysis (Figure 19(a)), artificial fiducial lines show a highly deformed structure near the surface. EDS confirmed that transfer of steel does not occur during this experiment. From the bending of the lines, the strain profile was determined. It fit well to an exponential function. Near the surface, the amount of strain is up to 3000%, whereas about 20μm below the surface, the displacement is almost negligible. A TEM micrograph (Figure 19(b)) after sliding at 180 m/s reveals that a nanocrystalline structure forms near the surface and extends about 1μm into the material. Below this nanocrystalline layer, heavily deformed flow structures were observed. Selected area diffraction patterns at each distinctive region confirm the presence of nanocrystalline structure. The width of the nanocrystalline region ranges from 50nm to several hundreds of nm.

Using FIB for preparation and TEM for observation, we observed two distinct regions (Fig. 20): a nanocrystalline region near the surface and more typical deformed structures further from the interface. However, FIB processing can lead to thermal effects that can modify the structure, especially in aluminum. Therefore we prepared another TEM foil by mechanical thinning, slurry drilling and jet polishing. Figure 21 shows a very highly deformed structure, even well below the surface.

FIB has the obvious advantage that it can produce foils with uniform thickness over a broad area, allowing convenient observation of cross-sections showing gradients of structure. However, because of thermal effects with FIB, our observations on these aluminum specimens suggest that conventional foil preparation techniques are less likely to modify the structure we want to study. Colleagues in another group at OSU have come to similar conclusions for their aluminum alloys.

Focused Ion Beam (FIB) is now used routinely to prepare site-specific specimens for TEM observation and analysis. However, a complementary technique, with a higher yield, takes advantage of ion-channeling contrast effects to obtain images in the FIB instrument itself. Ion contrast is shown in Figure 22(a) and a TEM micrograph is shown in Figure 22(b). Both images clearly show well-developed nanostructure near the friction surface and a pattern of

highly deformed material below it.

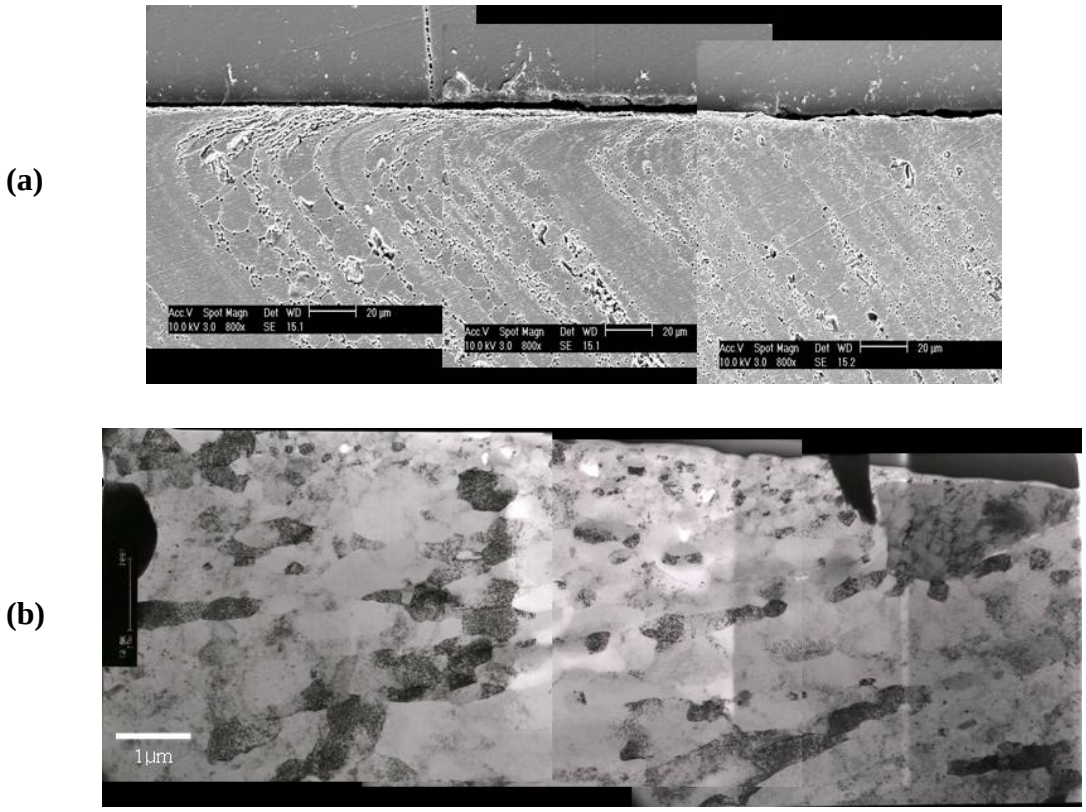

Fig. 19 **(b)** wing displacement profiles; (b) TEM image showing nanocrystalline structure adjacent to surface and extending about 1 µm from surface (180 m/s estimated sliding speed).

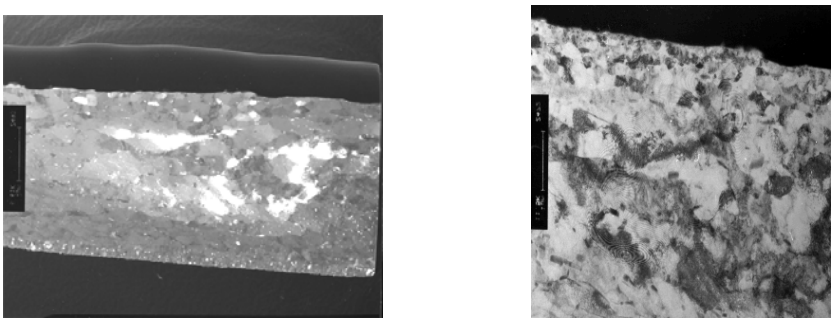

Fig. 20: TEM micrograph of (a) dark field image of whole area of thin membrane and (b) bright field image of higher magnification.

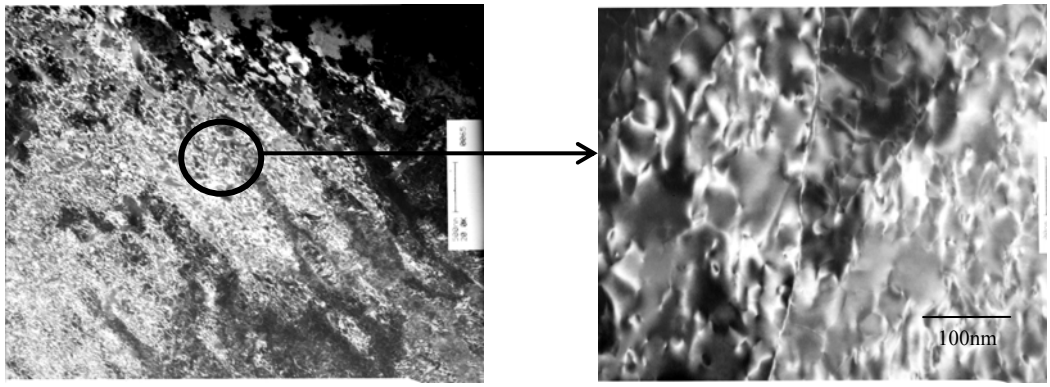

(a) (b)

Fig. 21: TEM micrographs of (a) highly deformed structure and (b) high magnification image of (a). Foil prepared by conventional methods (not FIB).

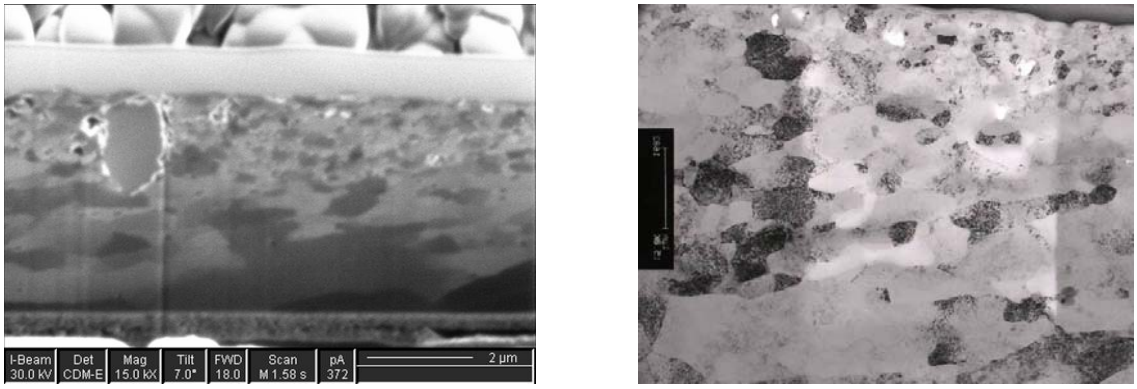

(a) (b)

Fig. 22: Comparison of cross-sections imaged (a) directly by ion contrast in the FIB instrument and (b) by TEM.

<u>Impact of Laboratory-wide problems at LANL</u>:

- The experimental part of the project being performed at LANL was suspended during the laboratory-wide shut-down. This stopped the production at LANL of impacted specimens that the OSU group was prepared to characterize.

- In November 2004, we petitioned to have the relevant portion of the lab re-opened so we could proceed with tests of impact with sliding. The petition was approved by the Director of LANL and by a Deputy Director of DOE. Soon afterwards, the LANL part of the team was allowed to resume experimental work on the project. One of our

students visited LANL during December, 2004. He received training and worked with the LANL team, but he was not authorized to perform impact tests. Since then, new specimens have been produced at LANL and mailed to OSU for characterization. Normal activities in the LANL RBGG lab did not resume during the remaining months of this project. Additional visits to LANL were planned but did not take place because of the problems at LANL.

- Details of the Lab-wide shut-down and the restart process are presented in Appendix 1 of this report. This Appendix has been updated for this final report.

- The delays at LANL forced us to re-focus our efforts at OSU. Fortunately, the OSU group built its own high-speed sliding instrument as part of this project, so tests and analysis have continued with that system. Also, the post-doc was able to devote more time to the application of fluid mechanics and MD simulations to the sliding behavior of both amorphous and crystalline materials. The results are intriguing and are contributing to major advances in understanding of velocity and strain rate dependence. The MD simulations exhibit formation of eddies (vorticity) and correlations with mechanical mixing. The mechanics calculations lead to new insight on the roles of strain rate sensitivity, which turns out to be a critical materials property. Further details of the simulations amd other calculations are provided later in this report.

Training:

The students were trained in the use of OSU's XL-30 Environmental Scanning Electron Microscope (ESEM), Pad-V X-Ray diffractometer, pin/disk wear testing apparatus, transmission electron microscope (TEM) sample preparation techniques and other characterization tools. Also, the post-doctoral researcher was trained in the use of our dual beam Focused Ion Beam (FIB) instrument, which enables the preparation of site-specific TEM samples. The students have been trained in the uses of the FIB instrument and received further experience with the TEM and with traditional specimen preparation involving electropolishing. The post-doctoral researcher learned to do molecular dynamics (MD) simulations of sliding, to analyze the results in terms of vorticity, and to combine fluid mechanics ideas with strain rate sensitivity to predict flow behavior near sliding interfaces.

Degree status of the two graduate students (Kim and Emge) is given in the earlier section on Project Personnel.

Computer Simulations and Other Analytic Work:

LANL: Theoretical and Simulation Synopsis

The development of theoretical understanding of frictional processes as a nonequilibrium phenomenon necessary to support the experimental work has been pursued at Los Alamos in the Applied Physics Division. This work supports the RBGG experiments in terms of modeling and interpretation of the velocity dependence and phase structure for the experimental results and their connection to other experiments in the High Energy Density Physics program. Some of this work has been presented (30-33 of Publications/Presentations list at end of this report).

Theoretical work associated with this project has been carried out by J. Hammerberg and his collaborators at Los Alamos National Laboratory (LANL). They have developed a model of dry sliding which incorporates mechanisms of microscopic dissipation that depend on the regime of sliding velocity, v, scaled by the transverse sound speed, c, of the weaker of the interfacial materials. For low values of v, $v/c << 1$, phonon mechanisms dominate and a linear response analysis leads to an initial increase in the frictional force with velocity for smooth interfaces. For higher velocities dislocation mechanisms become more important and for velocities $v/c \geq 1/10$, dynamically induced phase transformations occur resulting in a weakening of the frictional force with velocity and the formation of subgrain structure which may include local melting. In many cases the velocity dependence of the frictional force in this regime scales as $(v/c)^{-a}$, with $a = 3/4$. This theoretical and simulation background has been discussed in a series of publications and presentations. The constitutive theory of the frictional force outlined above is being compared with the experimental data that are being obtained in the pressure regime 0 to 5 GPa and velocity range 0 to 100 m/sec. Part of the theoretical program is numerical simulation of the experimental configuration via macroscopic computer simulations based upon the model described above.

OSU: Simulations and Theoretical Analysis Using Continuum Mechanics:

MD modeling at OSU began with simple amorphous materials to determine what features might be insensitive to details of structure. More recently the work has been extended to a simple crystalline network, with both smooth and rough interfaces. The presence of asperities affects the depth of the highly disturbed material. For both amorphous and crystalline cases, at high sliding speeds, the results suggest that the flow of material close to the sliding interface is characterized by the formation of eddies, intimate mixing and "diffusion-like" growth of the mixed layer. Vortices are a few nm in diameter. These eddies are largely responsible for frictional energy dissipation and mechanical mixing. Two examples of vorticity maps are shown in Figure 23.

The tribomaterial formed by vorticity is nanocrystalline or amorphous, depending on the system chosen. A comparison of eddy sizes with nanocrystal sizes in actual tribomaterial suggests that vorticity is directly responsible for the formation of such nanocrystal material. It is suggested that the flow of material near the interface is similar to that in fluids. The resulting eddies affect frictional energy dissipation and mechanical mixing. At lower sliding speeds the behavior is similar for amorphous materials but changes for crystalline materials. A shear-layer model of flow is qualitatively consistent with velocity profiles and friction behavior revealed by these MD simulations.

It is observed that the friction force is sensitive to velocity. This is attributed to the softening of the material due to localized heating resulting from sliding. This hypothesis is further supported by the concomitant attainment of steady state interface temperature and steady state friction. Flow properties appear to be highly sensitive to the temperature rise associated with frictional heating localized near the sliding interface. The response of crystalline and amorphous systems deviates at low velocities when crystalline systems with smooth interfaces do not undergo plastic deformation, thus leading to very low friction. This is in contrast to the behavior when asperities are present.

In addition to the simulation work, the application of fluid flow equations has been investigated. Similarities between material flow during sliding and fluid flow under Kelvin-Helmholtz instability are recognized and have been exploited to derive analytical models for velocity, strain-rate, strain and temperature profiles across the interface. Knowledge of strain-rate and strain profiles helps to define not only the region in which most of the deformation occurs, but also the rate of energy dissipation and the friction force. The analysis invokes

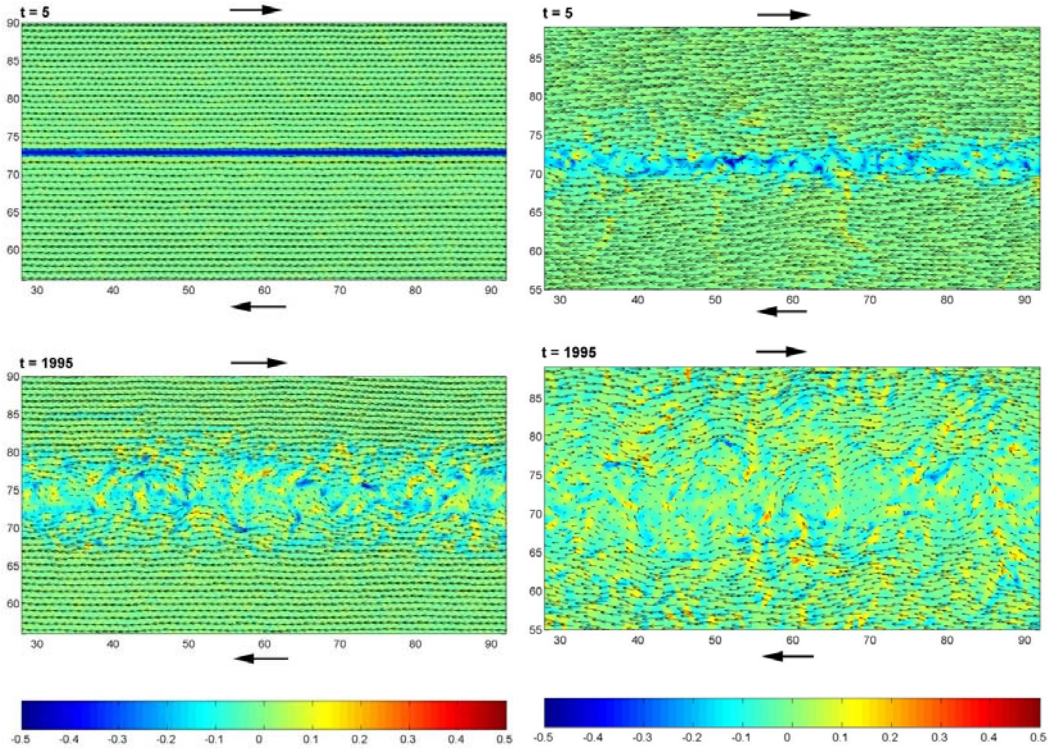

Fig. 23(a): Results from MD simulations of a model crystalline system A sliding on another crystalline system B at a relative velocity of 1.0 (Lennard-Jones units). Upper part of figure is at time t = 5, while lower part of figure is at t =1995. Shading represents vorticity. Velocity vector plots show development of vortices at sliding interface.

Fig. 23(b): Same as in (a) but for a model amorphous system. Note more extensive delocalization of vorticity than for the crystalline case.

momentum conservation principles and material flow laws to predict velocity profiles that develop during sliding. We assume a constant density and time-average flow only in the x-direction. Momentum balance considerations yield an equation like a diffusion equation. An effective viscosity can be defined and a generic flow law for a Herschel-Bulkley fluid brings in strength parameters and strain rate dependence. The solutions involve a Gauss hypergeometric function that includes strain rate sensitivity, m, as a materials parameter. The predicted velocity profile depends on the strain rate sensitivity, m. The spatial extent of the deformed zone is determined by strain rate sensitivity, strength parameters and the imposed sliding velocity. The analysis ought to apply for a wide range of size scales, from the nano-scale up to situations involved in plate tectonics. Preliminary results of this work were

published in Physical Review Letters, Sept. 2, 2005. Examples are shown in Figure 24. *These are very intriguing and important results that will be explored further during continuing DOE-sponsored research.*

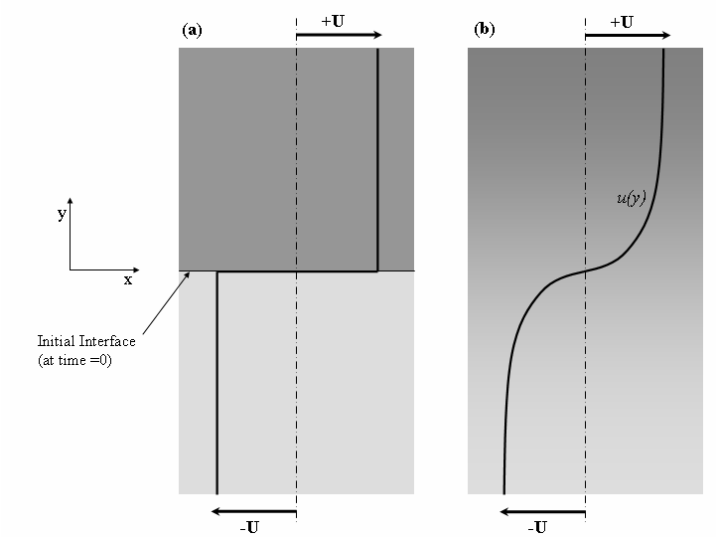

Fig. 24: Schematic showing velocity profile (bold) superimposed on sliding geometry consisting of two semi-infinite blocks. (a) Initially, blocks move rigidly at ± U with a sharp sliding interface. (b) Later, the interface becomes diffuse and a velocity profile evolves.

The principal equations used and derived are shown below:

Cauchy's equation of motion for this flow geometry is

$$\frac{\partial u}{\partial t} = \frac{1}{\rho} \cdot \frac{\partial}{\partial y}\left[\tau_{xy}\right], \qquad (1)$$

where τ_{xy} is the shear stress. The variation of density, *r*, across the interface is expected to be small and is neglected. By assuming a material flow law such as the Herschel-Bulkley model,

$$\tau_{xy} = \tau_0 + C \cdot \left(\frac{\partial u}{\partial y}\right)^m, \qquad (2)$$

where τ_0 and *C* are strength parameters, *m* is strain-rate sensitivity ($0 \le m \le 1$) and $\frac{\partial u}{\partial y}$ is shear strain rate. The general solution is a hypergeometric function, as shown below in equations (3)-(6):

$$u = \left(\frac{Cm(1+m)}{(1-m)\cdot\rho\cdot K_1}\right)^{\frac{1}{1-m}} \cdot \sqrt{2K_1} \cdot \hat{x} \cdot \left[{}_2F_1\left(\tfrac{1}{2}, \tfrac{1-3m}{2(1-m)} \mid \tfrac{3}{2} \mid \hat{x}^2\right)\right], \qquad (3)$$

where $\lambda \equiv \lambda \cdot \left(2K_1 + \lambda^2\right)^{-1/2}$. At $y = \pm\infty$, $y \cdot t^{\alpha} = \lambda = \pm\infty$ and $\lambda = \pm 1$ and it can be shown that

$$\lim_{\lambda \to 1} \lambda \cdot \left[{}_2F_1\left(\tfrac{1}{2}, \tfrac{1-3m}{2(1-m)} \mid \tfrac{3}{2} \mid \lambda^2\right)\right] = \frac{\Gamma(\frac{3}{2}) \cdot \Gamma(\frac{m+1}{2(1-m)})}{\Gamma(\frac{1}{1-m})} \equiv \Theta(m), \tag{4}$$

where Γ(β) is the gamma function of variable, β. Combining Eqs. (8), (9) and the BC at $y = \pm\infty$, gives

$$K_1 = \left[\frac{Cm(1+m)}{\rho(1-m)} \left(\frac{\sqrt{2} \cdot \Theta(m)}{U} \right)^{(1-m)} \right]^{\frac{2}{m+1}}. \tag{5}$$

Combining Eqs. (9) and (10) yields the velocity profile

$$u_n \equiv \frac{u}{U} = \frac{1}{\Theta(m)} \lambda \cdot \left[{}_2F_1\left(\tfrac{1}{2}, \tfrac{1-3m}{2(1-m)} \mid \tfrac{3}{2} \mid \lambda^2\right)\right]. \tag{6}$$

This function reduces to an error function solution for the case of m = 1 (Newtonian flow) and to an arctan function for the case of m = 0, which is close to the case for most metals (small values of m). When m = 1, the profile transition region increases with $t^{1/2}$, and when m = 0 it increases linearly with t. For intermediate cases, the increase is intermediate between these two cases. This analysis is being pursued for more realistic cases involving finite size specimens, work hardening, work softening and thermal effects.

Important implication: It should be noted that the strain rate sensitivity, m, enters into the solution for the velocity profile in many ways. The function F_1 depends directly on m, but so do the functions Θ(m), K_1 and $\hat{\lambda}$. *Therefore, the strain rate sensitivity emerges as a very important materials property for determining the development of the velocity profile during sliding. As such, it would appear to be a property that is key to understanding the evolution of sliding behavior.*

* * * * *

Publications/Presentations:

[1.] K.Subramanian, J.H.Wu and D.A. Rigney, The Role of Vorticity in the Formation of Tribomaterial during Sliding, presented at Spring MRS Meeting, San Francisco, April 12-16, 2004; published as paper 9.6 in MRS Procs. Vol. for Symposium P, Nanoscale Materials and Modeling—Relations Among Processing, Microstructure, and Mechanical Properties, 2004.
[2.] James E. Hammerberg and Brad Lee Holian, Surface Modification and Mechanisms: Friction, Stress, and Reaction Engineering, G.E.Totten and H.Liang, eds.,(Marcel Dekker, New York, 2004), pp.723-749.
[3.] J.E. Hammerberg, R. Ravelo, T.C. Germann, J.D. Kress and B.L. Holian, Shock

Compression of Condensed Matter-2003, M.D. Furnish, Y.M. Gupta, and J.W. Forbes, eds., (American Inst. of Physics, 2004), "Sliding Friction at Compressed Ta/Al Interfaces", pp. 565-568.
[4.] P. J. Crawford, K. N. Rainey, P. M. Rightley, and J. E. Hammerberg, 2003, "A Novel Experimental Technique for the Study of High-Speed Friction Under Elastic Loading Conditions," presented at the 13th American Physical Society Topical Conference on Shock Compression of Condensed Matter in Portland, OR, July 20-25, 2003, Proceedings edited by M. D. Furnish, Y. M. Gupta and J. W. Forbes, American Institute of Physics (2004), pp. 545-548.
[5.] James E. Hammerberg, Timothy C. Germann, Brad Lee Holian, and Ramon Ravelo, MRS Symposium Proceedings, Vol. 821: Nanoscale Materials and Modeling – Relations Among Processing, Microstructure and Mechanical Properties, " Nanoscale Structure and High Velocity Sliding at Cu/Ag Interfaces", p.6.5.1-p.6.5.6(2004), P.M.Anderson, T.Foecke, A.Misra and R.E.Rudd, eds., (Materials Research Society, Warrendale, PA).
[6.] J.E. Hammerberg, B.L. Holian, T.C. Germann and R. Ravelo, Metall. And Mat. Trans. 35A, "Nonequilibrium Molecular Dynamics Simulations of Metallic Friction at Ta/Al and Cu/Ag Interfaces", 2741-2745 (2004).
[7.] LANL Poster and presentation at DOE-NNSA workshop at Albuquerque, NM, March, 2004.
[8.] OSU Poster and presentation at DOE-NNSA workshop at Albuquerque, NM, March, 2004.
[9.] James E. Hammerberg and Brad Lee Holian, 'Simulation Methods for Interfacial Friction in Solids' in *Surface Modification and Mechanisms: Friction, Stress and Reaction Engineering*, G.E.Totten and H.Liang, eds., (Marcel Dekker, New York) 723-749 (2004).
[10.] J.E.Hammerberg and T.C.Germann, 'Frictional Interactions at Compressed Cu-Ag Interfaces', Plasticity-2005, Jan. 3-8, 2005, Kaua'i, HI.
[11.] H.-J. Kim, A. Emge, K. Subramanian and D. A. Rigney, Nanostructure Development Induced by Sliding Friction (poster), Ohio Nanotechnology Summit, Dayton, OH, March 2-3, 2005.
[12.] K. Subramanian and D. A. Rigney, Molecular Dynamics Study of Tribological Phenomena at High Sliding Velocities, APS March Meeting, Los Angeles, March 22, 2005.
[13.] P. J. Crawford, P. M. Rightley and J. E. Hammerberg, A Study of High Speed Friction Behavior under elastic Loading Conditions, APS March Meeting, Los Angeles, March 22, 2005.
[14.] R. Ravelo, T. C. Germann and J. E. Hammerberg, High Density, High Velocity Sliding for Ta, Al Interfaces, APS March Meeting, Los Angeles, March 22, 2005.
[15.] H.-J. Kim, A. Emge, S. Karthikeyan and D. A. Rigney, Effects of Tribooxidation on Sliding Behavior of Aluminum, presented at Intl. Conf. on Wear of Materials, San Diego, CA, April 24-28, 2005, and published in Wear 259 (2005) 501-505.
[16.] A. Emge, H.-J. Kim, K. Subramanian and D. A. Rigney, The Effect of Sliding Velocity on the Tribological Behavior of Copper, poster, presented at Intl. Conf. on Wear of Materials, San Diego, CA, April 24-28, 2005.
[17.] K. Subramanian and D. A. Rigney, Tribological Phenomena at High Sliding Velocities (poster), presented at Intl. Conf. on Wear of Materials, San Diego, CA, April 24-28, 2005, **Best Poster Award**.
[18.] LANL group plans to submit abstract to Shock Compression of Condensed Matter, APS Section Meeting, Summer, 2005.
[19.] LANL group plans to submit a paper on the RBGG (Cu/Cu, Cu/SS, Al/SS) to a refereed

journal by June, 2005 (consistent with a listed milestone for the friction project work package).
[20]. J.H.Wu, D.A. Rigney, M.L.Falk, J.H.Sanders, A.A.Voevodin, J.S.Zabinski, Tribological Behavior of WC/DLC/WS_2 Nanocomposite Coatings, Intl. conf. on Metallurgical Coatings and Thin Films, San Diego, CA, April 19-23, 2004; to be published in Surface and Coatings Technology, 2004.
[21.] J.H.Wu, S.Karthikeyan (same person as K.Subramanian), M.L.Falk, D.A.Rigney, Tribological Characteristics of Diamond-like Carbon (DLC) Based Nanocomposite Coatings, presented at Intl. Conf. on Wear of Materials, San Diego, CA, April 24-28, 2005, and published in Wear 259 (2005) 744-751. [Also, J.H.Wu attended Gordon Research Conf. on Tribology , Bristol, RI, June 27-July 2, 2004, and presented poster on related topics].
[22.] D. A. Rigney, invited as Keynote Speaker for the International Symposium on Forefront of Tribology, May 28-29, 2005, Kobe, Japan, "The Third Body Concept Updated: Plastic Flow, Accommodation of Shear, Velocity Profiles, Vorticity, Mechanical Mixing and Sliding Behavior."
[23.] D.A.Rigney invited as Keynote Speaker for the Symposium on Atomistics of Friction and Its Application for Nanotechnology, Intl. Tribology Conf. (ITC), Kobe, Japan, 2005. Authors: D.A.Rigney, J.H.Wu, K.Subramanian, M.L.Falk, What Can Simulations Tell Us about Tribophenomena in Real Materials?
[24.] D.A.Rigney, invited speaker at Kyunpook National University, Taegu, S. Korea, June 4, 2005, Three approaches to understanding sliding friction and wear.
[25.] D.A.Rigney, S. Karthikeyan, H.J.Kim, A. Emge, P. Rightley, J. Hammerberg, P. Crawford, Dynamic frictional events and the evolution of subsurface damage, Stewardship Science Academic Alliance (SSAA), Las Vegas, NV, August 23-25, 2005.
[26.] S. Karthikeyan, H. J. Kim and D.A. Rigney, Velocity and strain-rate profiles in materials subjected to Unlubricated sliding, Phys. Rev. Letters 95(Sept. 2, 2005), paper 106001.
[27.] D.A.Rigney, invited as Keynote Speaker for the Symposium on Wear and Fatigue of Materials, World Tribology Conference (WTC), Sept. 12-16, 2005, The Challenges of Sliding Wear.
[28.] H.J.Kim, A. Emge, S. Karthikeyan and D. A. Rigney, An Experimental and Theoretical Study of Microstructure Evolution during Sliding, Symposium on Integration of Theoretical, Computational and Experimental Studies of Interfaces and Microstructural Evolution, MS&T Conf., Pittsburgh, PA, Sept. 25-28, 2005; Procs. on CD, pp. 89-96.
[29.] H.J.Kim, A. Emge, S. Karthikeyan, D.A.Rigney, P. Keightley and R. Winter, Symposium on Ultrafine Grained Materials, TMS, San Antonio, TX, March 12-16, 2006, Nanostructure Formation Induced by Explosively Driven Friction, **Silver Medal Award** poster award.
[30.] P.J.Crawford, P.M.Rightley and J.E.Hammerberg, A Study of High Speed Friction Behavior under Elastic Loading Conditions, APS Annual Meeting, Los angeles, CA, 2005.
[31.] P.J.Crawford, P.M.Rightley, and J.E.Hammerberg, "Frictional Force Behavior in the Elastic Regime", Proc. 14th APS Topical Conference on Shock Compression of Condensed Matter, M.D. Furnish, Ed. (2006, to be published).
[32.] J.E.Hammerberg, R.Ravelo, and T.C.Germann, "High Density Sliding at Ta/Al and Al/Al Interfaces", Proc. 14th APS Topical Conference on Shock Compression of Condensed Matter – 2005, M.D.Furnish, Ed. (2006, to be published).

[33.] J.E.Hammerberg, T.C.Germann, R.Ravelo, and B.L.Holian, "Modeling Frictional Interactions at Ductile Metal Interfaces", Int. Conf. on New Models and Hydrocodes for Shock Wave Process in Condensed Matter, Dijon, France, April 9-14, (2006).

Planned Presentations:

[1.] D.A.Rigney, invited speaker, Gordon Research Conference, Colby College, Waterville, ME, June 18-23, 2006.
[2.] H.J.Kim, A.Emge, S.Karthikeyan and D.A.Rigney, Focused ion beam (FIB) analysis of structures induced by deformation during sliding, Gordon Research Conference (Tribology), Waterville, ME, June 18-23, 2006.
[3.] D.A.Rigney, invited plenary speaker, Tribology Symposium, Fifth Annual Congress, Brazilian Materials Research Society, Florianopolis, Brazil, October 8-12, 2006, Three approaches to understanding sliding friction and wear.
[4.] D.A.Rigney, invited keynote speaker, Symposium on Tribological Contacts: Fundamental Issues and Practical Solutions, MS&T Conf., Cincinnati, OH, Oct. 15-18, 2006, What is tribomaterial and how is it generated?
[5.] H.J.Kim, A. Emge, S. Karthikeyan, W.Windl and D.A.Rigney, Incorporation of oxygen during sliding of aluminum, Symposium on Tribological Contacts, Matls. Sci. & Technology, Cincinnati, OH, Oct. 15-19, 2006.
[6.] D.A.Rigney, invited plenary speaker, Intl. Conf. on Wear of Materials, Montreal, Quebec, Canada, April 15-19, 2007, Flow, Mixing and the Evolution of Tribomaterial.

Appendix 1

Lab-Wide Shut-Down of LANL and Restart Process
(updated May, 2006)

a. A Lab-wide shutdown of all work occurred on July 15, 2004. All work was given a 'risk level' and all work in DX division was declared 'risk level 3' – the highest level. To be cleared to each level required addressing safety and security issues, as determined by the lab Management Self-Assessment. For level 3 activities, a Laboratory Readiness Review involving LANL and DOE/NNSA oversight was required.

b. Nov 10, 2004. A memo drafted by OSU and the LANL team members was sent to the DX Division Leader. This memo detailed the urgency to restart the RBGG project.

c. Nov 17, 2004 DX-3 Group Leader performed a safety walk-down of the RBGG Friction Laboratory.

d. Nov 19, 2004 DX Division Leader (Acting) performed a safety walk-down of the

RBGG Friction Laboratory.

e. Nov 22, 2004 C-ADI Group Leader (Acting) performed a safety walk-down of the RBGG Friction Laboratory.

f. Nov 23, 2004 DX-division Waste Management coordinator performed a chemical/hazardous waste review of the RBGG Friction Laboratory.

g. As a result of the memo sent to the DX division management, it was decided to request a Level 0/3 Exemption, which would allow the operation of the RBGG Friction Lab as an "essential activity". This memo was initiated on Nov 22, 2005. After many revisions, the memo was sent to the Resumption Review Board (RRB). The RRB sent a recommendation to approve the request to the LANL Director and the Los Alamos Site Office of the NNSA on Dec 2, 2005.

h. Paul Rightley was informed of the approval of the Level 0/3 Exemption request by the LANL Director and the LASO on Dec 23, 2004.

i. Unfortunately, the holidays prevented any work from being conducted until Jan 1, 2005.

j. On Jan 24, 2005. Paula Crawford was converted to a regular staff member. As a result, work on the RBGG Friction project would become somewhat limited. This is due to the increased overhead cost of staff members as compared to post-docs.

k. Once the operation of the RBGG resumed, P. Crawford and P. Rightley worked to ensure smooth operation and collection of data.

l. Official collection of data was begun during the last half of Feb 2005.

m. Normal operation of the RBGG facility was expected to restart through the DX Division resumption process by the end of March 2005.

n. LANL team members in DX Division were reassigned to other tasks during 2005. Testing with the RBGG became dormant.

o. Communications between the OSU and LANL teams continued up to the present. Emails and phone calls were supplemented by letters sent by the P.I. (D. Rigney) to Dr. Paul J. Hommert, Division Leader, Applied Physics Division, and Dr. Kevin W. Jones, Division Leader, Dynamic Experimentation Division, on Sept. 26, 2005. These were supplemented by a petition letter sent by the P.I. on Feb. 13, 2006, to Dr. Dawn Flicker at LANL, who was considering budget constraints for a number of LANL programs. Subsequent email and phone calls during the winter and spring indicated optimism at LANL that the testing program with the RBGG facility would be able to proceed, thus providing a supply of specimens for the OSU team.